125. ESR-Spectroscopic Investigation of Radical Cations, Radical Anions, and Radical Trianions of Didehydro[n]annulenes

by **Walter Huber**

Institut für Physikalische Chemie der Universität Basel, Klingelbergstrasse 80, CH-4056 Basel

(25.IV.85)

The didehydro[n]annulenes **1** (n = 14), **2** (n = 18), and **3** (n = 22) are oxidized to radical cations. Reduction of the title compounds leads to radical anions and, in the case of **2** and **3**, to radical trianions. The hyperfine data of the paramagnetic derivatives are rationalized in terms of the occupation of n-membered (n = 14, 18, 22) π-perimeter MO's (HOMO, LUMO, NLUMO). The contact-ion pairs of the radical anions show unexpectedly large alkali-metal coupling constants.

Introduction. – The tetra(*tert*-butyl)didehydro[n]annulenes **1** (n = 14), **2** (n = 18), and **3** (n = 22), synthesized by *Nakagawa et al.* [1], are classified as *Hückel* aromatic compounds. These compounds are planar, relatively rigid and have a similar geometry of D_{2h} symmetry. Their 'aromatic character' is indicated by large diamagnetic ring-current effects, which, in accord with theoretical predictions [2], decrease with increasing ring size. Owing to the fact that properties of such annulenes depend critically on the number of π-electrons involved (*Hückel*'s rule [3]), characterization of the ionic derivatives obtained by reduction and oxidation is of special interest.

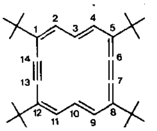

1

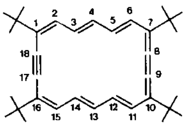

2

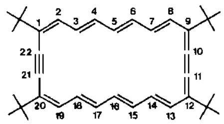

3

Based on the ESR-spectroscopic investigation of the respective radical anions $\mathbf{1}^{\cdot-}$–$\mathbf{3}^{\cdot-}$, *Gerson et al.* [4] have correlated the singly occupied MO with one of the doubly degenerate, lowest-antibonding MO's of a n-membered π-perimeter. In the course of our experiments, aiming at the preparation of novel ionic π-systems, we have recently converted the neutral $(4N + 2)\pi$-annulenes **1**–**3** into $(4N + 4)\pi$- $= (4N')\pi$-dianions and, subsequently, into $(4N + 6)\pi$- $= (4N' + 2)\pi$-tetraanions [5]. These conversions lead to large changes of the ring-current effects, which are relevant in verifying theoretical models. Here, we report on ESR- and ENDOR-spectroscopic investigations of the radical cations, radical anions, and radical trianions of the compounds **1**, **2**, and **3**. The ESR data are discussed in terms of the perimeter model and allow the characterization of the HOMO's (highest-occupied MO's), the LUMO's (lowest-unoccupied MO's), and the NLUMO's (next lowest-unoccupied MO's). Since the NMR investigations of the dianions show a large interdependence of ion pairing and ring-current effects [6], special attention is paid to the ion-pair structure of the negatively charged radicals.

Experimental. – The synthesis of the compounds **1**–**3** has been described by *Nakagawa et al.* [1]. The corresponding radical cations were prepared by reaction of the neutral compounds with $AlCl_3$ in CH_2Cl_2. The radical anions and the radical trianions were generated by reaction of the neutral compounds with K metal in THF. In a few experiments, DME, MTHF, and a mixture of DME/HMPT were used as the solvent. The radical anions were also prepared in Et_2O by employing Li, Na, K, and Cs metal as the reducing agent. ESR and ENDOR spectra of the paramagnetic derivatives of **1**–**3** were taken on a *Varian E-9-ESR* spectrometer with an attached *Varian-E-1700-ENDOR* unit.

Results. – *The Radical Cations of* **1**–**3**. The radical cations of **1**–**3** are long-lived and can be studied up to 300 K. In fact, well-resolved ESR spectra can only be observed above 220 K. *Fig. 1* shows the ESR spectra of **1**$^{+}$, **2**$^{+}$, and **3**$^{+}$ at 250 K. The pertinent coupling constants, a_{H_μ}, of the protons are determined from the ENDOR spectra and are confirmed by computer simulation of the ESR spectra *(cf. Table 1)*. The assignment of the values to sets of equivalent protons in **1**$^{+}$ is straightforward. It is also unambiguous for the pairs of equivalent protons and for the protons of the *t*-Bu groups in **2**$^{+}$ and **3**$^{+}$. The assignment of the remaining coupling constants to sets of four equivalent protons does not follow from experiment and is based on MO calculations *(cf. Discussion)*.

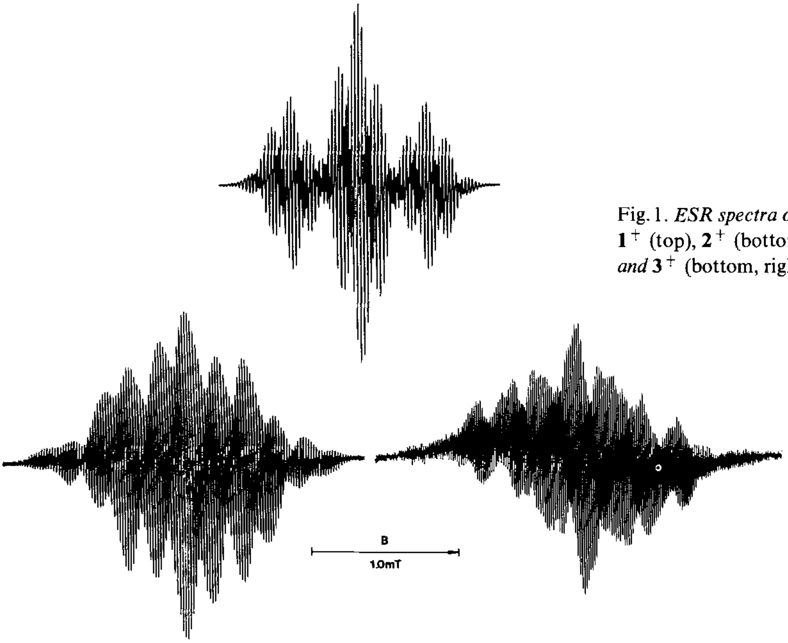

Fig. 1. *ESR spectra of the radical cations* **1**$^{+}$ (top), **2**$^{+}$ (bottom, left-hand side), *and* **3**$^{+}$ (bottom, right-hand side)

The Radical Anions of **1**–**3**. The ESR spectra of **1**$^{\cdot-}$, **2**$^{\cdot-}$ and **3**$^{\cdot-}$ in DME have been described in [4]. Our studies on the radical anions in THF by ESR and ENDOR spectroscopy are in agreement with these results. The proton coupling constants are not influenced by the change in the solvent from DME to THF *(cf. Table 1)*. Their assignment to sets of equivalent protons is based on the same arguments (multiplicity, MO calculation) as for the radical cations.

However, remarkable changes in the ESR spectra of the radical anions are observed in Et_2O as solvent. They are exemplified in *Fig. 2*, which shows the ESR spectra of **1**$^{\cdot-}$/K^{+} (K

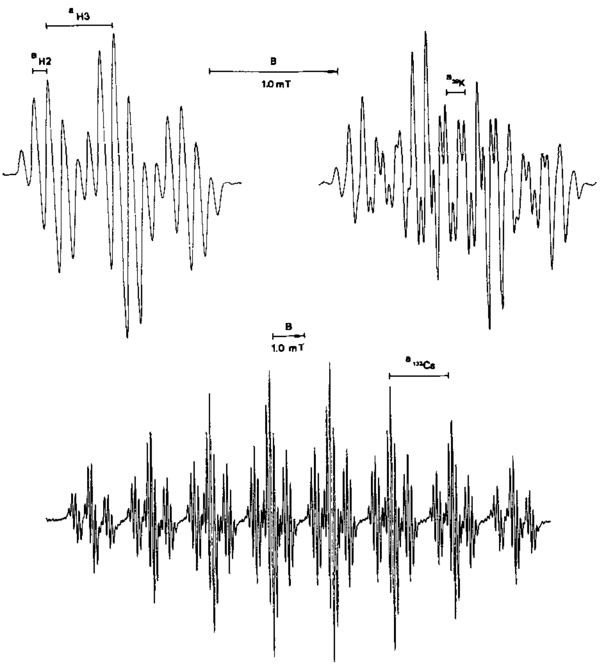

Fig. 2. *ESR spectra of* $\mathbf{1}^{\cdot-}/K^+$ *in THF* (top, left-hand side), $\mathbf{1}^{\cdot-}/K^+$ *in* Et_2O (top, right-hand side), *and* $\mathbf{1}^{\cdot-}/Cs^+$ *in* Et_2O (bottom)

salt) in THF and Et_2O as well as the ESR spectrum of $\mathbf{1}^{\cdot-}/Cs^+$ (Cs salt) in Et_2O. The prominent feature of the two latter spectra is the appearance of large alkali-metal coupling constants ($a_{^{39}K} = 0.235$ mT, $a_{^{133}Cs} = 1.92$ mT). Due to unresolved, second-order splitting, which stems from the ^{133}Cs-nucleus, the spacing between the groups of lines separated by a ^{133}Cs-coupling continuously increases on going from the low-field to the high-field end of the ESR spectrum (3.4%). The coupling constants of the ^{39}K- and the ^{133}Cs-nuclei show a significant temperature dependence (see *Table 2*). *Table 2* also includes ^{7}Li- and ^{23}Na-coupling constants of the respective alkali-metal salts of $\mathbf{1}^{\cdot-}$. The spectrum of $\mathbf{1}^{\cdot-}/Li^+$ deserves a special comment, being a superposition of two different ESR spectra. One of them (*ca.* 80%) is identical to the spectrum observed in THF as solvent, the other (*ca.* 20%) shows a ^{7}Li-coupling constant of 0.853 mT (210 K). The intensity of the latter spectrum is increased on raising the temperature.

In the spectra of the larger annulenes, alkali-metal coupling constants are only observed for the K salts ($\mathbf{2}^{\cdot-}/K^+$, $\mathbf{3}^{\cdot-}/K^+$) and the Cs salts ($\mathbf{2}^{\cdot-}/Cs^+$, $\mathbf{3}^{\cdot-}/Cs^+$). Their values, which are significantly smaller than those for the K and Cs salts of $\mathbf{1}^{\cdot-}$, are summarized in *Table 2*. It is obvious from *Table 1* that the proton coupling constants of the radical anions $\mathbf{1}^{\cdot-}$–$\mathbf{3}^{\cdot-}$ are only slightly influenced by going from THF to Et_2O as solvent.

The Radical Trianions of **2** *and* **3**. For **1**–**3**, the reduction proceeds beyond the radical anion stage. The formation of the diamagnetic dianions, which have been characterized by NMR spectroscopy [5], is indicated by the disappearance of the ESR spectra of $\mathbf{1}^{\cdot-}$–$\mathbf{3}^{\cdot-}$. In the case of **2** and **3**, further reduction on a K mirror leads to the appearance of new ESR spectra which are attributed to the corresponding radical trianions $\mathbf{2}^{3\cdot-}$ and $\mathbf{3}^{3\cdot-}$. As

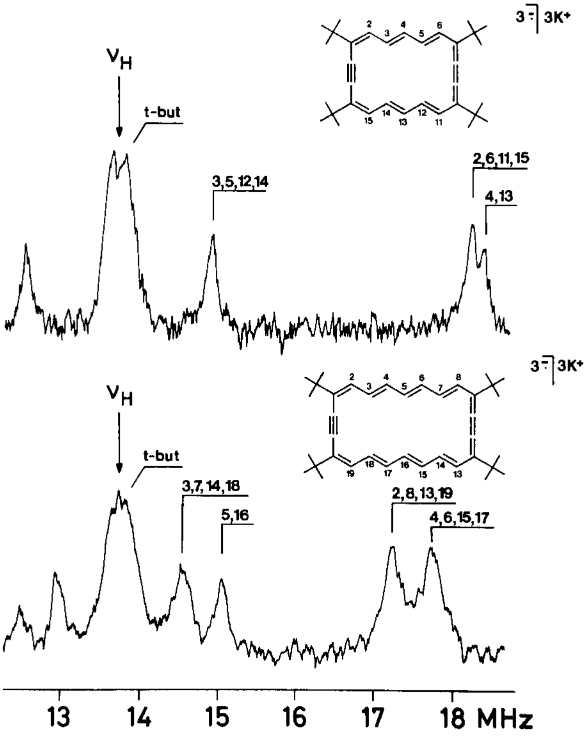

Fig. 3. *ENDOR spectra of* 2^{3-}/3K$^+$ *and* 3^{3-}/3K$^+$

expected from the molecular symmetry of **2** and **3**, the ENDOR spectra of $\mathbf{2}^{3-}$ and $\mathbf{3}^{3-}$ *(Fig. 3)* exhibit four and five absorption lines, respectively. The proton coupling constants for the trianions *(Table 1)* are derived from the positions of the ENDOR signals. They have been checked by simulation of the ESR spectra. Their assignment is based on the same arguments as those given for the radical anions and cations. The ESR spectra of $\mathbf{2}^{3-}$ and $\mathbf{3}^{3-}$ show no hyperfine splitting due to alkali-metal nuclei. However, one may assume that the large widths of the hyperfine lines are due to unresolved alkali-metal coupling constants. A detailed investigation on the influence of counterions and solvent on the ESR spectra of the trianions is inhibited by the fact, that conditions under which these highly charged species are studied can only be varied slightly. Limiting factors are their poor solubility and the low persistence. The problems are particularly acute in the case of the large counterion Cs$^+$ and with solvents of high solvating power (DME/HMPT). It is important to mention in this context that the ESR spectrum of $\mathbf{2}^{3-}$/3K$^+$ is not significantly changed on going from DME to MTHF as the solvent.

Discussion. – *Spin Distribution.* It has been demonstrated by *Gerson et al.* [4] that the simplest model which can be used to interpret the hyperfine data of the radical anions of **1**–**3** is that of a perturbed n-membered (n = 14, 18, 22) π-perimeter. *Fig. 4* represents schematically the two highest-bonding (Ψ_B) and the two lowest-antibonding (Ψ_A) MO's of a 14-, 18- and 22-membered π-perimeter. The perimeters are drawn to reflect the geometry of the corresponding didehydro[n]annulenes. The orbitals are classified as

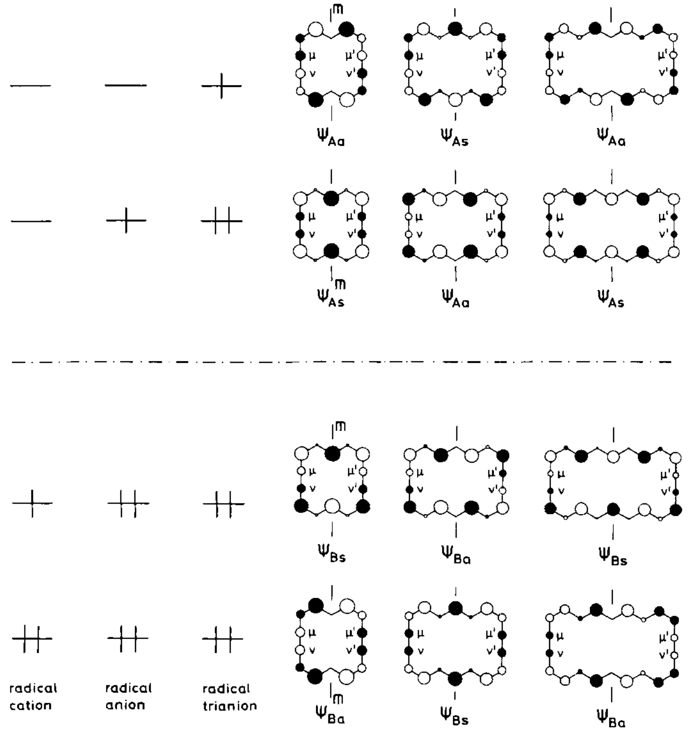

Fig. 4. *Schematic representation of the two highest-bonding* (Ψ_B) *and the two lowest-antibonding* (Ψ_A) *MO's of a 14-, 18- and 22-membered π-perimeter.* The orbitals are characterized as symmetric (Ψ_{Bs}, Ψ_{As}) or antisymmetric (Ψ_{Ba}, Ψ_{Aa}) with respect to the mirror plane m. The areas surrounded with circles are proportional to the square of the LCAO coefficients whereby blank and filled circles signify different signs.

symmetric (Ψ_{Bs}, Ψ_{As}) or antisymmetric (Ψ_{Ba}, Ψ_{Aa}) with respect to the mirror plane (m) *(Fig. 4)*.

Clearly, for the unperturbed n-membered perimeters of symmetry D_{nh}, the two bonding (Ψ_{Bs}, Ψ_{Ba}) and the two antibonding orbitals (Ψ_{As}, Ψ_{Aa}) are degenerate. However, for the didehydro[n]annulenes, the relative energies of these MO's will mainly be determined by the perturbation arising from the introduction of the two triple bonds (between centers μ–ν and μ'–ν').

For each of **1**–**3**, the predictions drawn from this model are fully borne out by the hyperfine data of the radical cation, radical anion, and radical trianion. Thereby, the singly occupied MO is unambiguously characterized by the magnitude of the coupling constant found for the pair of equivalent ring protons (positions 3,10 in **1**, 4,13 in **2** and 5,16 in **3**). These protons lie either in the nodal plane of the singly occupied MO (antisymmetric type orbitals Ψ_{Ba} and Ψ_{Aa}) or are attached to centers with large LCAO coefficients (symmetric type orbitals Ψ_{Bs} and Ψ_{As}). The pairing properties of the HOMO and LUMO can be verified by comparison of the coupling constants of the radical anions and the radical cations [7].

Taking the paramagnetic derivatives of **2** as an example, one readily recognizes the similarity of the coupling constants of $\mathbf{2}^{+}$ and $\mathbf{2}^{-}$. This finding clearly indicates that the

HOMO and the LUMO of **2** possess similar LCAO coefficients. In both **2**$^{+}$ and **2**$^{\cdot-}$, the magnitude of the coupling constant found for the pair of equivalent ring protons in the 4,13-positions (0.129 and 0.135 mT in **2**$^{+}$ and **2**$^{\cdot-}$, respectively) is relatively small, indicating the single occupancy of the antisymmetric orbitals (Ψ_{Ba}- and Ψ_{Aa}-like orbitals) with a nodal plane through the relevant centers 4,13, as predicted by the simple model above. The NLUMO in **2** is characterized as Ψ_{As}-like by the large magnitude of the coupling constant of the protons at the centers 4,13 (0.334 mT).

Table 1. *Experimental and Calculated Coupling Constants* (in mT) *of the Radical Ions of* **1**, **2**, *and* **3**

	t-Bu	2	3	4	5
1^{+}[a]	0.019	0.106 (+0.136)[b]	0.462 (−0.520)		
2^{+}[a]	0.018	0.086 (+0.090)	0.394 (−0.404)	0.129 (+0.138)	
3^{+}[a]	0.016	0.069 (+0.062)	0.328 (−0.323)	0.123 (+0.115)	0.364 (−0.345)
1$^{\cdot-}$[c]	< 0.01[e]	0.108	0.514		
1$^{\cdot-}$[d]	< 0.01[e]	0.111 (+0.136)	0.494 (−0.520)		
2$^{\cdot-}$[c]	< 0.01[e]	0.087	0.402	0.135	
2$^{\cdot-}$[d]	< 0.01[e]	0.087 (+0.090)	0.392 (−0.404)	0.122 (+0.138)	
3$^{\cdot-}$[c]	< 0.01[e]	0.064	0.337	0.124	0.399
3$^{\cdot-}$[d]	< 0.01[e]	0.058 (0.062)	0.347 (−0.323)	0.134 (+0.115)	0.397 (−0.345)
2$^{3\cdot-}$[c]	< 0.01[e]	0.325 (−0.310)	0.120 (0.078)	0.334 (−0.432)	
3$^{3\cdot-}$[c]	< 0.01[e]	0.250 (−0.216)	0.057 (+0.041)	0.287 (−0.333)	0.093 (+0.091)

[a] Oxidized with $AlCl_3$ in CH_2Cl_2.

[b] Values in brackets are coupling constants calculated by the HMO-*McLachlan* procedure ($\lambda = 1.2$) [8] and the *McConnell* relationship ($Q = -2.5$ mT) [10].

[c] Solvent: THF; counterion: K^+; $T = -80°$.

[d] Solvent: Et_2O; counterion: K^+; $T = -80°$.

[e] Values estimated from the ENDOR line-width.

In an HMO-*McLachlan*-type calculation [8] of the spin distribution used for the assignment of the coupling constants to sets of four equivalent protons, the integral of the triple bonds ($\beta_{\mu\nu} = \beta_{\mu'\nu'}$) is set equal to 1.5β. The remaining HMO parameters retain their standard values α and β. No allowance was made for the substituent effect of the *t*-Bu groups, in view of the nearly identical coupling constants observed for the corresponding ring protons in **1**$^{\cdot-}$ (0.514, 0.108 mT) and the unsubstituted radical anion (0.515, 0.115 mT) [9]. The calculated π-spin populations are converted into coupling constants by the use of the *McConnell* relationship [10]. As is obvious from *Table 1*, such calculated values correlate very well with the experimental values in the case of **1**$^{\cdot-}$–**3**$^{\cdot-}$ and **1**$^{+}$–**3**$^{+}$. A slightly poorer correlation is found for the large coupling constants in the radical trianions **2**$^{3\cdot-}$ and **3**$^{3\cdot-}$. This finding might be due to the interaction of the highly charged species with the counterion which is not accounted for by the model calculation.

Ion Pairing. A remarkable finding is the occurrence of extremely large alkali-metal coupling constants, especially in the case of **1**, when the radical anions are generated under conditions which favor contact ion pairs (*e.g.* Et_2O as the solvent). Alkali-metal coupling constants as observed for **1**$^{\cdot-}$ in Et_2O have not yet been reported for radical anions of pure hydrocarbons: *e.g.*, the ^{39}K-coupling constant of **1**$^{\cdot-}$/K^+ is larger by a factor of 30 than the coupling constant which occurs in the contact-ion pair of the anthracene radical anion [11]. The coupling constants are even larger than those observed in the case of chelates which are formed by the radical anion of *o*-dimesitoylbenzene and alkali-metal cations (0.375, 0.695, 0.133 and 1.02 mT for the ^7Li-, ^{23}Na-, ^{39}K-, and the ^{133}Cs-nucleus) [12].

Table 2. *Alkali-Metal Coupling Constants* a_M *Observed in the ESR Spectra of* **1**$^{\cdot-}$, **2**$^{\cdot-}$, *and* **3**$^{\cdot-}$ *in* Et_2O *as the Solvent and Calculated s-Spin Populations* ρ_M

	1$^{\cdot-}$ a)		**1**$^{\cdot-}$ b)		**2**$^{\cdot-}$ a)		**2**$^{\cdot-}$ b)		**3**$^{\cdot-}$ b)	
	a_M c)	ρ_M d)	a_M	ρ_M	a_M	ρ_M	a_M	ρ_M	a_M	ρ_M
^7Li	0.853	0.059	0.913	0.064	c)		c)		c)	
^{23}Na	0.776	0.025	0.781	0.029	c)		c)		c)	
^{39}K	0.235	0.029	d)		0.045	0.006	0.078	0.009	0.060	0.007
^{133}Cs	1.920	0.023	2.081	0.025	0.691	0.008	0.655	0.008	0.388	0.005

a) T = –60°.
b) T = 0°.
c) Alkali-metal coupling constant not observed.
d) Due to the low resolution, the ESR spectrum of **1**$^{\cdot-}$/K^+ at 0° can not be analyzed.

The temperature dependence of the alkali-metal coupling constants observed for the ion pairs of **1**$^{\cdot-}$–**3**$^{\cdot-}$ points towards fast equilibria between solvent separated and contact-ion pair. An exceptional case is, however, the Li salt of **1**$^{\cdot-}$ for which the tight and the 'free' or loosely associated radical anion give rise to concurrently superimposed signals in the ESR spectrum. Obviously, in the Li salt the change from a solvent separated to a contact-ion pair is slow on the hyperfine time-scale. This finding might be rationalized by a tighter solvation of Li^+ by the Et_2O solvent. Comparably low exchange rates have been reported for alkali-metal salts of some cyclophane radical anions [13].

The finding that the spin distribution observed for the contact-ion pairs still reflects the original symmetry of the didehydro[n]annulenes is most significant. It indicates that the counterion assumes an equilibrium position above (or below) the molecular plane in the center of the monocycle. Such a location of the counterion should be favored for electrostatic and steric reasons. One can show by a simple HMO calculation that the π-centers 3,10 in **1**$^{\cdot-}$ and 5,16 in **3**$^{\cdot-}$ bear the highest negative-charge density. The situation is slightly different in the contact-ion pairs of **2**$^{\cdot-}$. The analogous π-centers 4,13 in **2**$^{\cdot-}$ are situated in a nodal plane of the singly occupied MO (see *Fig. 4*). High negative-charge density is found on the neighboring centers 3,14 and 5,12. From electrostatic and MO-theoretical reasons, it is thus straightforward to assume that in the contact-ion pairs of **2**$^{\cdot-}$ the counterion is preferentially localized in an unsymmetrical position between the centers 3,14 or 5,12. The occurrence of a symmetrical spin distribution must then be rationalized by a fast fluctuation of the counterion between these two equivalent positions. A similar model of ion pairing has been suggested for contact-ion pairs of the naphthalene radical anion [14]. The role of steric requirements on the location of the counterion relative to the π-system is quite obvious. Due to the bulkiness of the four *t*-Bu substituents the counterions can best approach the negatively charged π-system in the middle of the monocycle.

In comparing the interactions of a given radical anion with different counterions, the spin density transferred into the s-orbitals of the alkali-metal cations can be taken as a measure. The observed coupling constants (a_M) are, therefore, converted into s-spin populations (ρ_M) by using *Eqn. 1* [15], where a_o^{ns} represents the coupling constant of the free alkali metal [16].

$$\rho_M = a_M/a_o^{ns} \qquad (1)$$

From the amount of the spin density ρ_M, it is straightforward to assume, that $\mathbf{1}^{\overline{\cdot}}$ possesses a perfect perimeter size and a singly occupied MO of appropriate symmetry for an interaction with the alkali-metal cations. It is, however, important to mention, that the ρ_M-values obtained within the series of contact-ion pairs of $\mathbf{1}^{\overline{\cdot}}$ are not strongly suggestive of an interdependence of cationic radius and cation-anion interaction. Although the radius of the counterion significantly increases on going from the Na to the Cs salt of $\mathbf{1}^{\overline{\cdot}}$, the pertinent s-spin population on the alkali-metal cations remains nearly constant. The remarkably large value observed for the Li contact-ion pair does not necessarily indicate an enhanced cation-anion interaction. The rationalization of this spin population has to consider the low ratio between solvent separated and contact-ion pairs. Based on the concentration ratio of these two species (80% solvent separated and 20% contact-ion pairs), one calculates a spin population of 0.012 for a hypothetical fast-exchanging species. This value is significantly lower than the values obtained for the other alkali-metal salts of $\mathbf{1}^{\overline{\cdot}}$.

The assumption that $\mathbf{1}^{\overline{\cdot}}$ possesses the perfect structural prerequisites for the association with alkali-metal cations gains further significance by taking into account the contact-ion pairs of the larger annulenes. Certainly, the increasing delocalization of the negative charge in the larger π-systems leads to a weakening of the cation-anion interaction. This effect, however, can not be solely responsible for the drastic decrease in ρ_M-values observed on going from the contact-ion pairs of $\mathbf{1}^{\overline{\cdot}}$ to those of $\mathbf{2}^{\overline{\cdot}}$ and $\mathbf{3}^{\overline{\cdot}}$. It seems highly probable, that – with respect to $\mathbf{1}^{\overline{\cdot}}$ – the overlap of the π- and the atomic orbitals is seriously reduced in contact-ion pairs of $\mathbf{2}^{\overline{\cdot}}$ and $\mathbf{3}^{\overline{\cdot}}$, due to the enlarged π-perimeter and the nodal properties of the singly occupied MO's.

The existence of the highly charged radical trianions as contact-ion pairs seems beyond any doubt. This conclusion is supported by the low persistence of $\mathbf{2}^{3\overline{\cdot}}$ and $\mathbf{3}^{3\overline{\cdot}}$ in solvents of high cation-solvating power (*e.g.* DME/HMPT). Unfortunately, the ESR spectra of $\mathbf{2}^{3\overline{\cdot}}$ and $\mathbf{3}^{3\overline{\cdot}}$ in THF provide no information about the number of associated counterions or the structure of the associates. The absence of large alkali-metal coupling constants can probably be rationalized by the nodal properties of the singly occupied MO (NLUMO). In contrast to the LUMO's, the NLUMO's of **2** and **3** possess several nodal planes which pass (or are nearby) the center of the perimeter. From steric and electrostatic arguments, one would suggest an ion-pair structure for the trianions with alkali-metal cations localized over the centre of the negatively charged π-system. Due to the above mentioned nodal properties of the NLUMO's, these positions are highly unfavorable for a direct spin transfer from the singly occupied orbitals into the atomic orbitals of the alkali-metal cations.

Financial support of this work by the *Swiss National Science Foundation* and *Ciba-Geigy AG, Sandoz AG* and *F. Hoffmann-La Roche & Cie AG,* Basel, is greatly appreciated. The author is grateful to *Prof. M. Nakagawa* and *M. Iyoda* for samples and to *Prof. F. Gerson* for helpful discussions.

REFERENCES

[1] K. Fukui, T. Nomoto, S. Nakatsuji, M. Nakagawa, *Tetrahedron Lett.* **1972,** 3157; M. Iyoda, M. Nakagawa, *ibid.* **1972,** 4253; M. Iyoda, M. Nakagawa, *J. Chem. Soc., Chem. Commun.* **1972,** 1003.

[2] M. J. S. Dewar, G. J. Gleicher, *J. Am. Chem. Soc.* **1965,** *87,* 685.

[3] E. Hückel, *Z. Phys.* **1931,** *70,* 204.

[4] F. Gerson, J. Jachimowicz, M. Nakagawa, M. Iyoda, *Helv. Chim. Acta* **1974,** *57,* 2141.

[5] K. Müllen, W. Huber, T. Meul, M. Nakagawa, M. Iyoda, *J. Am. Chem. Soc.* **1982,** *104,* 5403.

[6] K. Müllen, W. Huber, T. Meul, M. Nakagawa, M. Iyoda, *Tetrahedron* **1983,** *39,* 1575.

[7] E. Heilbronner, H. Bock, in 'Das HMO-Modell und seine Anwendung', Verlag Chemie, GmbH, Weinheim, 1968, pp. 132–150.

[8] A. D. McLachlan, *Mol. Phys.* **1960,** *3,* 233.

[9] N. M. Atherton, R. Mason, J. Wratten, *Mol. Phys.* **1966,** *11,* 525.

[10] H. H. McConnell, *J. Chem. Phys.* **1956,** *24,* 632.

[11] H. Nishigushi, Y. Nakai, K. Nakamura, K. Ishizu, Y. Deguchi, H. Takaki, *Mol. Phys.* **1965,** *9,* 153.

[12] B. J. Herold, A. F. Neiva Correia, J. dos Santos Veiga, *J. Am. Chem. Soc.* **1965,** *87,* 2661.

[13] F. Gerson, *Topics Curr. Chem.* **1983,** *115,* 57.

[14] L. Pedersen, R. G. Griffin, *Chem. Phys. Lett.* **1970,** *5,* 373.

[15] W. Lubitz, M. Plato, K. Möbius, R. Biehl. *J. Phys. Chem.* **1979,** *83,* 3402.

[16] J. P. Goldsborough, T. P. Kohler, *Phys. Rev. A* **1964,** *133,* 135.